Treatment of Collinear and Noncollinear Electron Spin within an Approximate Density Functional Based Method†

Christof Köhler* and Thomas Frauenheim

Bremen Center for Computational Materials Science, Bremen University, 28359 Bremen, Germany

Ben Hourahine

SUPA, Department of Physics, University of Strathclyde, John Anderson Building, 107 Rottenrow, Glasgow G4 0NG, United Kingdom

Gotthard Seifert

Technische Universität Dresden, Institut für Physikalische Chemie und Elektrochemie, 01062 Dresden, Germany

Michael Sternberg

Center for Nanoscale Materials, Argonne National Laboratory, 9700 South Cass Avenue, Building 440, Argonne, Illinois 60439-4812

Received: December 21, 2006; In Final Form: February 14, 2007

We report benchmark calculations of the density functional based tight-binding method concerning the magnetic properties of small iron clusters (Fe_2 to Fe_5) and the Fe_{13} icosahedron. Energetics and stability with respect to changes of cluster geometry of collinear and noncollinear spin configurations are in good agreement with ab initio results. The inclusion of spin−orbit coupling has been tested for the iron dimer.

1. Introduction

The density functional based tight-binding method (DFTB)[1] together with its later self-consistent charge extension (SCC−DFTB)[2] were originally developed for closed-shell systems. Both approaches are computationally very efficient approximations to fully self-consistent Kohn−Sham density functional theory, and successful applications include a wide range of problems in the fields of molecules including biomolecules, surfaces, and interfaces as well as point and extended defects in solid-state systems.[3,4]

In this work, we will present in its entirety an extension of the SCC−DFTB method toward the inclusion of spin-polarization effects in a collinear[3−5] as well as noncollinear description, the latter for the first time. We will also give first results concerning an inclusion of spin−orbit coupling effects. This extends the applicability of the DFTB approach in principle toward systems containing isolated spin-polarized transition metal ions, i.e., in functional centers of biomolecules, transition metal clusters, and magnetic bulk systems and to the calculation of isotropic hyperfine coupling constants of materials containing unpaired electrons.[6]

The collinear DFTB approach has been previously tested extensively for the magnetic and structural properties of iron clusters.[5,7,8] While conventional density functional theory (DFT) treatments are currently limited to about 25 unique atoms in a cluster, especially if a scanning of the potential energy hypersurfaces is included, the spin-polarized DFTB method (SDFTB) has successfully been applied to up to 147 unique atoms in the Fe_{147} icosahedron.

These size limitations of DFT become even more severe once noncollinear spin systems with their increased number of degrees of freedom have to be taken into account. These are supposed to play a role in several transition metal systems.

Nonferromagnetic spin arrangements have been reported for manganese,[9] chromium,[10] and iron[10−14] clusters, transition metal overlayers,[15] as well as solid-state systems, i.e., a spin−spiral ground state has been reported for γ-iron.[16,17] Here, the noncollinear SDFTB might provide a viable alternative to gain insight into the qualitative magnetic behavior of much larger systems than possible with DFT.

Our paper is organized as follows. In Section 2, we will introduce the SDFTB approach in its collinear and noncollinear formulation and will present ideas concerning the treatment of spin−orbit effects. Some test results for collinear spin configurations in iron clusters will briefly be summarized in Section 3 before proceeding with new benchmark results on noncollinear spin configurations in small iron clusters (Fe_2 to Fe_5) and the Fe_{13} icosahedron comparing to DFT. We will also report results for spin−orbit coupling in the Fe_2 molecules.

2. Method

The collinear as well as the noncollinear formulation of the SDFTB method are obtained from a expansion of the spin-polarized Kohn−Sham (KS) total energy[18−20] around reference densities. While in the collinear case, the wavefunctions involved in the KS total energy expression are diagonal in spin space, in the noncollinear case, the wavefunctions are two-component

† Part of the "DFTB Special Section".

* Corresponding author. E-mail: c.koehler@bccms.uni-bremen.de.

10.1021/jp068802p CCC: $37.00
Published on Web 04/12/2007

spinors. However, the basic approximations leading to the SDFTB method[4,5] can be readily obtained in the collinear case without the additional complication from the use of two-component spinors. Therefore, we will first present the collinear SDFTB method before proceeding to the noncollinear case and then spin−orbit coupling as extensions to it.

A. Collinear Spin. With the total electron density $n(\vec{r}) = n_\uparrow(\vec{r}) + n_\downarrow(\vec{r})$ and the magnetization density $m(\vec{r}) = n_\uparrow(\vec{r}) - n_\downarrow(\vec{r})$ as basic variables, the spin-polarized collinear KS total energy expression reads: |

$$E_{\mathrm{tot}}^{\mathrm{KS}} = \sum_{\sigma=\uparrow,\downarrow}\sum_{i}^{\mathrm{occ}} n_{i\sigma}\left\{\left\langle\psi_{i\sigma}\right| -\frac{\nabla^2}{2} + v_{\mathrm{ext}} + \frac{1}{2}\int \frac{n(\vec{r}\,')}{|\vec{r}-\vec{r}\,'|}\,\mathrm{d}^3r'\left|\psi_{i\sigma}\right\rangle\right\} + E_{xc}[n(\vec{r}), m(\vec{r})] + \frac{1}{2}\sum_{IJ}^{M}\frac{Z_I Z_J}{|\vec{R}_I-\vec{R}_J|} \quad (1)$$
$$E_{NN}$$

In eq 1, M is the number of nuclei in the system that each carry an atomic charge of Z_I.

Similarly to the approach of Foulkes and Haydock,[21] we expand the total electron density and the magnetization density around reference densities n_0 and m_0:

$$n(\vec{r}) = \sum_{\sigma=\uparrow,\downarrow}\sum_{i}^{N} n_{i\sigma}|\psi_{i\sigma}|^2 = n_0(\vec{r}) + \delta n(\vec{r})$$
$$m(\vec{r}) = m_0(\vec{r}) + \delta m(\vec{r}) \qquad \text{with } m_0 = 0 \quad (2)$$

where δn and δm are fluctuations in these densities. The reference for the magnetization density is the nonmagnetic case, which in turn is the state described by the SCC−DFTB formalism.[2] With this choice of variables and reference points, the spin polarization becomes a correction on top of the established SCC−DFTB method, which is fully recovered in the case of a vanishing magnetization density fluctuation, e.g., a nonspinpolarized system.

Insertion of eq 2 into the total energy expression of eq 1, Taylor expansion of the exchange-correlation contribution and approximation of the resulting integrals, finally leads to the SDFTB total energy expression (for details, see refs 4,5):

$$E_{\mathrm{tot}} = \sum_{\sigma=\uparrow,\downarrow}\sum_{i}^{\mathrm{occ}} n_{i\sigma}\langle\psi_{i\sigma}|\hat{H}_0[n_0,0]|\psi_{i\sigma}\rangle + \frac{1}{2}\sum_{A}^{M}\sum_{B}^{M}\sum_{l\in A}\sum_{l'\in B}\Delta q_{Al}\Delta q_{Bl'}\gamma_{Al,Bl'} + E_{\mathrm{rep}} + \frac{1}{2}\sum_{A}\sum_{l\in A}\sum_{l'\in A} p_{Al}p_{Al'}W_{All'} \quad (3)$$

Deviating from the usual SCC−DFTB formulation, we resolve the Hubbard U in the algebraic function $\gamma(\vec{R}_A,\vec{R}_B,U_{Al},U_{Bl'})$ with respect to atom and angular momentum shell. The Δq_{Al} are then the differences between the atomic reference charges (q^0) and the Mulliken populations q_{Al} per atom A and angular momentum l, defined as $\Delta q_{Al} = q_{Al} - q_{Al}^0$.

This is necessary to describe the difference between the 3d electrons and the 4s and 4p electrons as encountered in the valence of third row transition metals, see Section 2E and Section 3. Choosing common Hubbard parameters for electrons with the same principal quantum number reduces possible problems with the definition of the Hubbard U for an empty atomic orbital.[22] For atoms with valence electrons of only a single principal quantum number, this also leads to the conventional SCC−DFTB treatment with one Hubbard U per atomic species.

The p_{Al} in eq 3 are the Mulliken spin-population differences per atom A and angular momentum l

$$p_{Al} = q_{Al\uparrow} - q_{Al\downarrow} \quad (4)$$

while the atomic constants $W_{All'}$ can be calculated as

$$W_{All'} = \frac{1}{2}\left(\frac{\partial\epsilon_{l\uparrow}}{\partial n_{l'\uparrow}} - \frac{\partial\epsilon_{l\uparrow}}{\partial n_{l'\downarrow}}\right) \quad (5)$$

Here, the $\epsilon_{l\uparrow}$ are the atomic eigenvalues and $n_{l'\uparrow}$ are the occupation numbers of the atomic orbitals of the species A. The actual values are given in Section 2E.

Expansion of the wavefunction $|\psi_{i\sigma}\rangle$ into a linear combination of atomic orbitals, see ref 3 for details, and variation of eq 3 with respect to the expansion coefficients $c_{vi\sigma}$ leads to the Hamiltonian matrix elements of the SDFTB approach:[5]

$$\hat{H}_{\mu\nu\sigma} = \hat{H}^0_{\mu\nu} + \frac{1}{2}S_{\mu\nu}\sum_{C}^{M}\sum_{l''\in C}(\gamma_{A(\mu)l(\mu),Cl''} + \gamma_{B(\nu)l(\nu),Cl''})\Delta q_{Cl''} + \delta_\sigma\frac{1}{2}S_{\mu\nu}\Big(\sum_{l'\in B(\mu)} W_{B(\mu)l(\mu)l'}p_{B(\mu)l'} + \sum_{l'\in B(\nu)} W_{B(\nu)l(\nu)l'}p_{B(\nu)l'}\Big). \quad (6)$$

An analytic expression for the forces can be obtained by differentiation of the total energy expression in eq 3 with respect to the nuclear coordinates.[5]

B. Noncollinear Spin. The collinear formulation of SDFTB is given for magnetic quantization with respect to the z direction (i.e., projected into up and down populations with respect to z). In systems where effects like spin−orbit coupling or hindering of spin interactions (such as antiferromagnets with a triangular lattice) are significant, the direction of spin quantization can vary in space. Additionally, even for purely collinear spin systems, it is desirable to be able to write the SDFTB expressions so that they are rotationally invariant with respect to changes in the quantization direction.

The original spin-polarized local-density approximation of von Barth[20] gives such a rotationally invariant form, where the magnetization density is vectorial instead of scalar. If we write the wavefunctions of the system as two-component spinors instead of scalar wavefunctions, the total electron and magnetization densities are then given as linear combinations of Pauli matrices

$$\vec{n}(\vec{r}) = \sum_{i}^{N} n_i\begin{pmatrix}\psi_i^\alpha\\ \psi_i^\beta\end{pmatrix}^*\begin{pmatrix}\psi_i^\alpha\\ \psi_i^\beta\end{pmatrix} \quad (7)$$

$$= n(\vec{r})\begin{pmatrix}1&0\\0&1\end{pmatrix} + m^x(\vec{r})\begin{pmatrix}0&-i\\ i&0\end{pmatrix} + m^y(\vec{r})\begin{pmatrix}0&1\\1&0\end{pmatrix} + m^z(\vec{r})\begin{pmatrix}1&0\\0&-1\end{pmatrix} \quad (8)$$

$$= n(\vec{r}) + \vec{m}(\vec{r}) \quad (9)$$

Hence the Kohn−Sham Hamiltonian without spin−orbit term is[23]

$$H = \nabla^2 + v[n(\vec{r})] + v_{xc}[n(\vec{r}),\vec{m}(\vec{r})]. \tag{10}$$

To define the Mulliken charges used in the DFTB method, a straightforward generalization of the spinless Mulliken analysis for spinor wavefunctions is given by

$$q_\mu^{\alpha\beta} = \sum_i \sum_\nu n_i S_{\mu\nu} c_{i\mu}^{\alpha} * c_{i\nu}^{\beta} \tag{11}$$

$$= q_\mu \begin{pmatrix} 1 & 0 \\ 0 & 1 \end{pmatrix} + p_\mu^x \begin{pmatrix} 0 & -i \\ i & 0 \end{pmatrix} + p_\mu^y \begin{pmatrix} 0 & 1 \\ 1 & 0 \end{pmatrix} + p_\mu^z \begin{pmatrix} 1 & 0 \\ 0 & -1 \end{pmatrix} \tag{12}$$

so the density becomes quaternion-like with a vectorial spin.

Because the exchange-correlation potential must be locally parallel to the spin-polarization vector[24] (or at least the part that can be evaluated with existing functionals), we write the noncollinear SDFTB energy (without spin−orbit or external fields) directly as

$$E_{\text{tot}}^{\text{noncoll}} = \sum_{\alpha\beta} \sum_i^{\text{occ}} n_i \langle \psi_i^\alpha | \hat{H}[n_0,0] | \psi_i^\beta \rangle + \frac{1}{2} \sum_A^M \sum_B^M \sum_{l\in A} \sum_{l'\in B} \Delta q_{Al} \Delta q_{Bl'} \gamma_{Al,Bl'} + E_{\text{rep}} + \frac{1}{2} \sum_A^M \sum_{l\in A} \sum_{l'\in A} \vec{p}_{Al} \cdot \vec{p}_{Al'} W_{All'} \tag{13}$$

which in the limiting case of collinear spin simplifies to spin vectors that are purely along one axis. In the case of z quantization, this becomes eq 3, hence the spin constants, W, are the same as in the collinear treatment.

The magnetic part of the energy is similar to Pickett's orthogonal tight-binding implementation of noncollinear spin.[25] Variation of eq 13 with respect to the wavefunction coefficients leads to the noncollinear Hamiltonian, which is conveniently written as spin superblocks:

$$\hat{H}_{\mu\nu} = \left\{ \hat{H}_{\mu\nu}^0 + \frac{1}{2} S_{\mu\nu} \sum_C^M \sum_{l''\in C} (\gamma_{A(\mu)l(\mu),Cl''} + \gamma_{B(\nu)l(\nu),Cl''}) \Delta q_{Cl''} \right\} \begin{pmatrix} 1 & 0 \\ 0 & 1 \end{pmatrix} + \left\{ \frac{1}{2} S_{\mu\nu} \right\} \left[\sum_{l'\in B(\mu)} W_{B(\mu)l(\mu)l'} \begin{pmatrix} p_{B(\mu)l'}^z & p_{B(\mu)l'}^y - i p_{B(\mu)l'}^x \\ p_{B(\mu)l'}^y + i p_{B(\mu)l'}^x & -p_{B(\mu)l'}^z \end{pmatrix} + \sum_{l'\in B(\nu)} W_{B(\nu)l(\nu)l'} \begin{pmatrix} p_{B(\nu)l'}^z & p_{B(\nu)l'}^y - i p_{B(\nu)l'}^x \\ p_{B(\nu)l'}^y + i p_{B(\nu)l'}^x & -p_{B(\nu)l'}^z \end{pmatrix} \right] \tag{14}$$

with again a secular equation

$$\sum_\nu \begin{pmatrix} c_{\nu i}^\alpha \\ c_{\nu i}^\beta \end{pmatrix} \left[\begin{pmatrix} \hat{H}_{\mu\nu}^{\alpha\alpha} & \hat{H}_{\mu\nu}^{\beta\alpha} \\ \hat{H}_{\mu\nu}^{\alpha\beta} & \hat{H}_{\mu\nu}^{\beta\beta} \end{pmatrix} - \epsilon_i S_{\mu\nu} \begin{pmatrix} 1 & 0 \\ 0 & 1 \end{pmatrix} \right] = 0 \tag{15}$$

where the overlap is spin independent.

Similarly, the forces are given by differentiating the total energy (eq 13) with respect to atomic coordinates.

C. Constraints on Spin Directions. Often, spin configurations other than the ground (or other stationary) state of the noncollinear expressions are of interest. For example, to compare the FM and AFM configurations discussed in section 3 requires nonground state configurations. To obtain self-consistent solutions for these excited spin configurations, the constrained DFTB formalism discussed in ref [26] has been also applied for spin configurations. Unlike previous spin constraints in DFT,[27] the external potential is obtained from maximization of a functional with respect to undetermined multipliers of the form suggested by Wu and Van Voorhis.[28]

The generalized DFTB energy expression then becomes

$$W = E_{\text{tot}}^{\text{noncoll}} + \sum_i \lambda_i [\sum_\nu (\vec{w}_{i\nu} \cdot \vec{p}_{i\nu}) - \sigma_i] \tag{16}$$

where $E_{\text{tot}}^{\text{noncoll}}$ is the noncollinear total energy (eq 13), λ_i is the ith for the constraining direction given by $\vec{w}_{i\nu}$. W is convex in $n(r)$ and concave in λ, allowing the variational optimization of the undetermined multipliers. The constrained form of the noncollinear Hamiltonian is again constructed by taking variations with respect to wavefunction coefficients. The addition to the Hamiltonian is of the form

$$\hat{H}_{\mu\nu}^{\text{constr}} = \left\{ \frac{1}{2} S_{\mu\nu} \right\} \sum_i \lambda_i \left[\begin{pmatrix} w_{i\mu}^z & w_{i\mu}^y - i w_{i\mu}^x \\ w_{i\mu}^y + i w_{i\mu}^x & -w_{i\mu}^z \end{pmatrix} + \begin{pmatrix} w_{i\nu}^z & w_{i\nu}^y - i w_{i\nu}^x \\ w_{i\nu}^y + i w_{i\nu}^x & -w_{i\nu}^z \end{pmatrix} \right] \tag{17}$$

D. Spin−Orbit Coupling. The Pauli form of the Hamiltonian is also useful when including spin−orbit coupling. The mean-field single-particle on-site spin−orbit interaction can be written in the form

$$\vec{L} \cdot \vec{S} = \frac{1}{2} \begin{pmatrix} \hat{L}_z & \hat{L}_- \\ \hat{L}_+ & -\hat{L}_z \end{pmatrix} \tag{18}$$

$$\hat{H}^{\text{SO}} = \xi \vec{L} \cdot \vec{S} \tag{19}$$

$$E_{\text{SO}} = \sum_i n_i \sum_\nu \sum_\mu \hat{H} \nu c_{\mu i \mu}^{\text{SO}*} c_{i\nu} \tag{20}$$

These matrix elements are given in closed form in ref 29. For simplicity, we have followed the empirical tight-binding approach of using precomputed spin−orbit constants.[30] An example of this method applied to the splittings of the Si band structure is given in Table 1. For on-site only spin−orbit, this does not introduce any additional contributions to the forces. For the calculations on the Fe structures, as with the work of Pastor et al., we take the 3d spin−orbit coupling constant to be 50 meV.[31] For the isolated Fe atom, the spin is found to be 4.0 μ_B, while the orbital moment is found to only be 0.29 μ_B, which substantially underestimates the atomic orbital moment of 2.0 μ_B. Similar underestimates of orbital moments are typically present in LDA/GGA and tight-binding calculations, including spin−orbit, and often rectified with orbital polarization

TABLE 1: Spin−Orbit Splittings (eV) of the Si Band Structure at Γ and *L* Compared against (a) Empirical Tight-binding[30] and (b) Experiment[34] [a]

Si	Chadi (a)	DFTB	expt (b)
$\Delta\Gamma_{7v-8v}$	0.045	0.045	0.044
$\Delta\Gamma_{7c-8c}$	0.05	0.086	0.04
$\Delta L_{6v-4c,5v}$	0.03	0.034	0.02
$\Delta L_{6c-4c,5c}$	0.03	0.066	0.03

[a] The same spin−orbit constant as the empirical tight-binding is used.

TABLE 2: Numerical Values in Atomic Units of the $W_{All'}$ Constants Used in This Work

		s	p	d
Fe	s	−0.016	−0.012	−0.003
($3d^74s^1$)	p	−0.012	−0.029	−0.001
	d	−0.003	−0.001	−0.015

corrections[32,33] (these have not been applied for the results presented here).

E. Technical Details. The Hamiltonian matrix elements $\hat{H}^0_{\mu\nu}$ and overlap matrix elements $S_{\mu\nu}$ of the SDFTB were tabulated using a $3d^74s^1$ excited reference configuration for the iron atom, similar to previous DFT[36] and DFT pseudopotential[35] calculations.

The complete Hubbard U's for the iron atom in atomic units are $U_{4s} = 0.20$, $U_{4p} = 0.15$, and $U_{3d} = 0.36$, but we use the U_{4s} value for the U_{4p} as well as discussed in Section 2A, except when noted otherwise in case of the Fe_5, see Section 3B1.

The spin constants $W_{All'}$ used in this work are given in Table 2 from DFT/PBE calculations. These constants, and similarly the Hubbard U,[3] are obtained from numerical differentiation of the KS eigenvalues with respect to the occupation numbers, see eq 5, the numerical accuracy is $\leq 1 \times 10^{-2}$ although we give more digits for the $W_{All'}$.

To maintain better control we have not automatically optimized the geometries of the clusters using the SDFTB forces, e.g., with a steepest descent approach, except for the noncollinear Fe_5 cluster, see Section 3B1. Instead, the bond lengths were varied in 0.1 Å steps (retaining symmetry) to obtain the bond lengths corresponding to the total energy minimum, which we report in Table 3. For Fe_{13}, the cluster volume was changed in 2% steps as indicated below.

3. Application

A. Collinear Calculations. The SDFTB method has previously been applied to the magnetic properties of iron clusters. Up to Fe_{32}, the potential hypersurfaces have been searched with a genetic algorithm,[5] while around Fe_{55}, Fe_{110} and Fe_{147} selected clusters were studied.[7,8] Comparing with DFT/LSDA results, which are available up to Fe_{17}[35] (referenced as DFT/PSP in this article), we find excellent agreement concerning the energetically most favorable cluster structures and their respective magnetic moments if the different Hubbard U's are taken into account.[37]

To demonstrate this, we give in Figure 1 the magnetic moments of the energetically most favorable iron clusters up to Fe_{13} from different approaches. We note that the SDFTB method gives the same energetically most favorable structures as the DFT/PSP[35] reference in this size range.

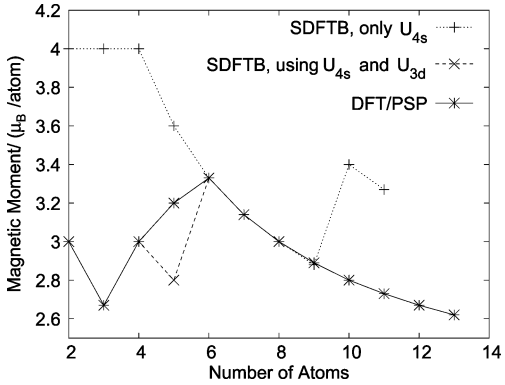

Figure 1. Magnetic moments for the energetically most favorable iron clusters up to Fe_{13} from SDFTB and DFT/PSP[35] calculations. The SDFTB using U_{4s} and U_{3d} as detailed in Section 2E overlay the DFT/PSP results except for Fe_5. The SDFTB results using only the single U_{4s} for all orbitals show large deviations from either.

The ground-state magnetic moment of the clusters in the SDFTB approach were obtained by varying the number of unpaired electrons in integer steps, e.g., the discretization step is $2\mu_B$. The difference between the angular momentum resolved SDFTB and the DFT/PSP reference result for Fe_5 is exactly one discretization step. For the other cluster sizes, there is an exact agreement between the two calculations.

However, using only the 4s Hubbard U in the SDFTB calculations leads to a large overestimation of magnetic moments compared to the DFT/PSP reference. Especially for the very small clusters with 2−4 atoms, this SDFTB calculation gives erroneous magnetic moments of 4 μ_B/atom, corresponding to the maximal possible number of unpaired electrons in an iron atom. This is an effect of the energy gain due to the spin polarization coupled with, according to the Mulliken analysis, an excitation of electrons between atomic shells that is not countered by a SCC contribution to the total energy. Only if different Hubbard U values for U_{4s} and U_{3d} are used, is there a non-negligible SCC contribution countering the intershell charge transfer in these homonuclear clusters.

For the Fe_{13} icosahedron, which is the energetically most favorable cluster of this size, a ferromagnetic and an antiferromagnetic spin configuration are known from collinear[14] and

TABLE 3: Noncollinear SDFTB Results for Small Iron Clusters.

molecule	configuration	bond lengths, Å	magnetic moment, μ_B/atom	E_{tot}, eV
Fe_2	FM	2.2	3.15 (3.15)	−72.25
	AFM	2.3	±3.21 (0.00)	−71.26
Fe_3, C_{3v}	FM	2.3	2.71 (2.71)	−110.97
Fe_3, D_{3h}	FM	2.3	3.55/2.90 (3.33)	−109.53
	AFM	2.2	±3.58/0.00 (2.39)	−108.76
Fe_4, T_d	FM	2.3/2.4	3.00 (3.00)	−150.61
Fe_4, C_{4v}	FM	2.3	3.50 (3.50)	−149.50
Fe_4, D_{4h}	FM	2.3/2.5	3.61/3.39 (3.5)	−146.38
	AFM	2.3/2.5	±3.67/± 3.47 (0.00)	−146.46
Fe_5, D_{3h}	FM	2.3	2.73/2.91 (2.80)	−189.93
	NC	2.5	(±1.94,2.73,0.00) (3.4) (0.00,3.36,0.00)	−190.01
	FM, relaxed	2.33/2.49	2.77/2.85 (2.8)	−190.46

[a] For Fe_2, Fe_3, and Fe_5, only a completely symmetrical cluster has been considered, while for Fe_4, a symmetry-breaking analogue to the DFT/PAW reference[10] has been introduced. For the FM and AFM states, the total moment is given in parenthesis. For the FM and relaxed FM state of Fe_5, the magnetic moments of the two unique atoms of the trigonal bipyramid are given. For the NC state of Fe_5, the magnetic system is of C_2 symmetry, with the vector spins of the two apical atoms given.

noncollinear[11] calculations. A detailed discussion concerning this is presented in Section 3B2 using the noncollinear SDFTB approach.

B. Noncollinear Calculations. *1. Fe_2 to Fe_5.* Noncollinear calculations on small iron clusters up to Fe_5 with DFT were performed by Hobbs et al. using the projector-augmented wave (PAW) formalism.[10] We will refer to this work as DFT/PAW throughout this paper. Evidence of antiferromagnetic as well as noncollinear spin arrangements, especially for Fe_5 (trigonal bipyramidal geometry), has been obtained,[10] but a later study[11] employing a GGA density functional found a collinear ground state if taking a distortion of the geometry into account. All studies[10,11,14] hint to a delicate dependence of the cluster ground state on the density functional and volume.

We performed constrained SDFTB calculations, see Section 3C, for some isomers of Fe_2 to Fe_5 and the Fe_{13} icosahedron. In a first step, the magnetization vectors associated with each atom as well as their magnitude were constrained to DFT/PAW reference values to have a defined starting point. In the second step, the constraints have been relaxed completely. This yields the final unconstrained magnitudes and directions of the magnetic moment vectors. Unlike in the collinear calculations presented in Section 3A, the magnitude of the spin components can now vary smoothly.

The results for Fe_2 to Fe_5 are summarized in Table 3 for different ferromagnetic (FM), antiferromagnetic (AFM), and noncollinear (NC) states.

For the iron dimer, we calculated the energy difference between the FM and AFM state with 0.5 eV/atom, which compares well to noncollinear DFT/PAW reference data, giving 0.65 eV/atom in GGA and 0.75 eV/atom in LDA.

The central atom of the Fe_3 linear chain carries a smaller moment of 2.90 μ_B/atom compared to the outer atoms with 3.55 μ_B/atom each in the FM configuration, while its magnetic moment vanishes completely in the AFM spin configuration. The outer atoms then have opposite magnetic moments with a magnitude of 3.58 μ_B/atom, similar to the AFM configuration for Fe_2.

For the linear chain geometrical arrangement of Fe_3, we find the AFM state to be energetically less favorable compared to the FM state by about 0.26 eV/atom, which is in qualitative agreement with the DFT/PAW reference, which estimates the energy difference to be about 0.13 eV/atom in GGA. However, the LDA result of the DFT/PAW reference reverses this, with the AFM state being the energetically most favorable one by again about 0.13 eV/atom. This highlights the error bar introduced by different approximations for the exchange-correlation functional even in fully self-consistent DFT treatments.

Only collinear FM and AFM states are present on the SDFTB energy surfaces for Fe_3. This is similar to the DFT/PAW results, where energetically unfavorable NC arrangements are present using a GGA density functional but vanish if the LDA is used.

For Fe_4, the DFT/PAW data suggest a symmetry breaking between the two pairs of atoms leading to two different bond lengths. In the SDFTB results, we find that this is not as pronounced as in the DFT/PAW. For the linear chain arrangement, the bond lengths between the inner two atoms is the larger one.

For the tetrahedral and rectangular geometries of Fe_4, FM spin configurations could be stabilized for several distances. The tetrahedral cluster is the energetically most favorable one of the two by about 0.28 eV/atom. The two bond lengths in the tetrahedron do not differ as much as in the DFT/PAW reference.

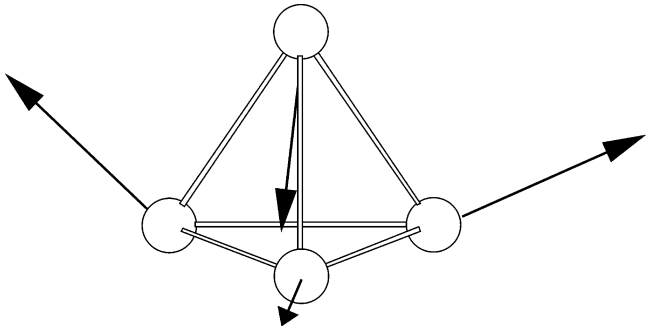

Figure 2. Noncollinear magnetic moment vectors in the tetrahedral Fe_4 cluster.

The energetically unfavorable noncollinear spin arrangement described in the DFT/PAW work for the tetrahedral Fe_4 cluster could not be stabilized in the SDFTB calculations but collapses into the FM spin configuration except for a bond length of 2.5 Å. For this fully symmetric geometry, a noncollinear spin configuration with a total energy of −149.17 eV exists. The magnetic moment vectors of length 3.33 μ_B are displayed in Figure 2. The angle between the vectors is about 109.5°, consistent with the angles in a tetrahedron.

The Fe_4 linear chain has an AFM configuration within the SDFTB approach with the two dimers carrying opposite magnetic moments and which is energetically slightly more favorable than the FM configuration. This energetic ordering is reversed compared to the DFT/PAW reference data. However, in both cases, the energy differences between the two spin configurations are in the range of only about 0.1 eV, which is small compared to the energy differences to the tetrahedral and rectangular geometries which are about 1 eV/atom.

For the symmetric trigonal bipyramidal Fe_5 cluster, we find in agreement with the DFT/PAW reference data a noncollinear spin arrangement to be more stable than the FM one by about 0.02 eV/atom. The magnetic moments of the capping atoms are slightly distorted from the FM arrangement, the absolute values of the vector components are comparable to the DFT/PAW data.

It has been pointed out in the literature that this noncollinear ground state might be stabilized by not taking Jahn−Teller distortions into account.[11] Relaxing the cluster geometry using the noncollinear SDFTB starting from the noncollinear spin configuration without constraints leads in fact to a slightly distorted configuration with FM spin configuration, denoted as "FM, relaxed'' in Table 3.

We would also like to note that the exact angle of the magnetization vectors in the NC arrangement depends somewhat on the choice of Hubbard U's in the SDFTB Hamiltonian. Although Mulliken analysis shows that the noncollinear vector component is, like the collinear one, dominantly a d-shell contribution, repeating the calculation with the U_p different from U_s reduces it from about 1.9 μ_B to about 0.4 μ_B. The magnitude of the vectors in the FM arrangement changes only by about 0.01 μ_B using this procedure, which is the magnitude also observed in collinear SDFTB calculations for various clusters.

Summarizing the SDFTB method in its noncollinear formulation gives results in good qualitative agreement with DFT/PAW data for Fe_2 to Fe_5. The data on noncollinear arrangements for these small clusters is in particularly good agreement with the LDA reference data.

2. Fe_{13} Icosahedron. The Fe_{13} icosahedron has been the subject of several DFT studies using collinear as well as noncollinear approaches because of concurrent AFM and FM

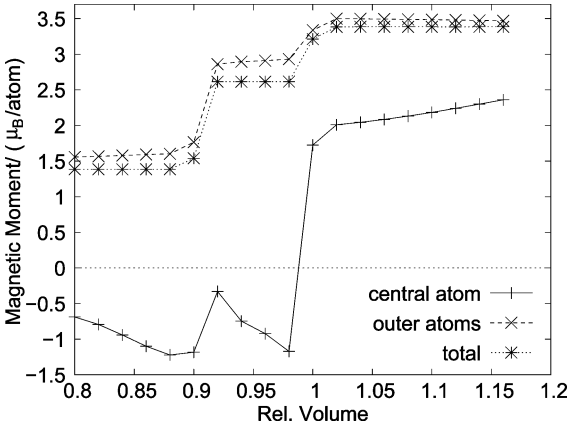

Figure 3. Magnetic moments in the Fe_{13} icosahedron using a FM start configuration.

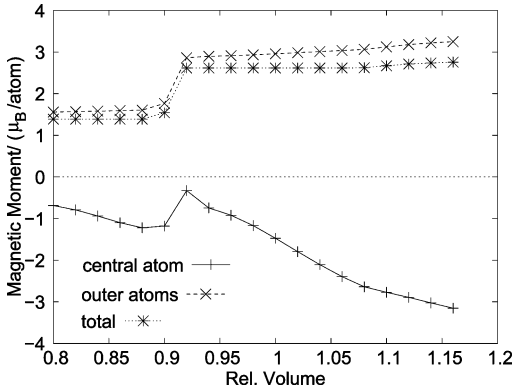

Figure 4. Magnetic moments in the Fe_{13} icosahedron using an AFM start configuration.

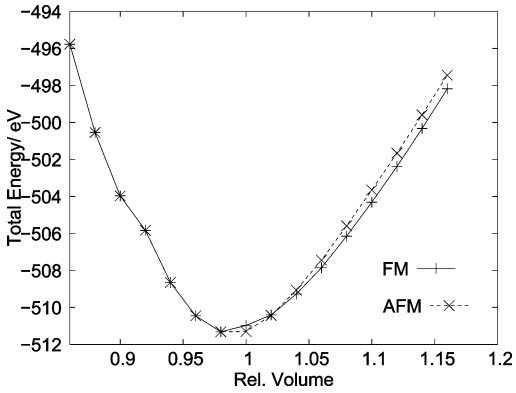

Figure 5. Total energy of the Fe_{13} icosahedron for the spin states obtained from FM and AFM start configurations, see Figures 3 and 4.

spin configurations in this cluster.[11,14] We have performed SDFTB calculations starting from a fully symmetric cluster structure with a bond length of 2.56 Å between outer-shell atoms and 2.43 Å from the outer-shell atoms to the central atom. This will constitute the reference volume denoted "1.00" in Figures 3, 4, and 5 for the subsequent steps. To scan the potential energy hypersurface, we changed the cluster volume in 2% steps by scaling the atom coordinates of the shell atoms. The relative volume 0.8 corresponds to a distance of 2.05 Å between outer-shell atoms and 1.95 Å from an outer-shell atom to the central atom. These distances are 2.97 and 2.83 Å for a relative volume of 1.16, respectively.

For every volume, AFM and FM initial configurations were prepared using constraints and a self-consistent solution found. After that, the constraints were completely removed to obtain the final magnetic moments in the cluster using a noncollinear description. These final unconstrained magnetic moments are shown in Figures 3 and 4, respectively.

Up to a relative volume of 0.98, we obtain the same spin configuration from both initial states in our calculation. After that, the two sets of calculations start to diverge, as we will now discuss in detail.

The outer-shell atoms have a positive magnetic moment regardless of the initial configuration. Starting from a FM initial configuration, Figure 3, one obtains three distinct steps in the absolute value of the magnetic moment of the 12 outer-shell atoms: from about 1.6 μ_B/atom to about 2.8 μ_B/atom and then again to its maximum value of about 3.4 μ_B/atom. If the calculation is initialized with an AFM configuration, Figure 4, for the outer-shell atoms, only the first two values are observed. The total magnetic moment of the cluster changes similarly.

The magnetic moment of the central atom can assume positive and negative values depending on the relative volume and the initial spin configuration.

For relative volumes smaller than 1.00, its magnetic moment, Figure 4, is negative, with an absolute value of not more than about 1.3 μ_B regardless of the initial spin configuration.

For relative volumes larger than or equal to 1.00, the final magnetic moment of the central atom depends on the starting configuration. With the FM initial configuration, Figure 3, the final magnetic moment is positive but smaller than on the outer-shell atoms. Initializing with an AFM spin configuration, the final magnetic moment of the central atom is negative with a maximum absolute value of about 3 μ_B for a relative volume of 1.16, see Figure 4. In the latter case, the third step in the magnetization of the outer-shell atoms is missing as mentioned above. Instead, the magnetic moment on the outer-shell atoms increases smoothly with the cluster's relative volume from the (with respect to Figure 3) intermediate value of about 2.8 μ_B/atom to about 3.2 μ_B/atom.

In summary, from the magnetic moments in Figures 3 and 4, one can distinguish two different final AFM spin configurations and one final FM spin configuration.

The total energies of the spin states in Figures 3 and 4 are given in Figure 5. For relative volumes ≤ 0.98, the two curves are identical because the same final spin configuration is obtained. For a relative volume of 1.00, the AFM solution is the energetically more favorable one in SDFTB by about 0.33 eV total or 0.025 eV/atom. However, this changes for larger volumes where the FM end configuration becomes energetically more favorable with the crossover point at about a relative volume of 1.02.

Again, the SDFTB results are in good agreement with DFT/LSDA data showing exactly these effects of the cluster volume on the magnetic configuration[14] and in good qualitative agreement with respect to the magnetic moments at the reference volume to noncollinear DFT/GGA data.[11] However, the smallness of the energy difference between the two states, whether obtained from SDFTB or DFT,[11,14] highlights the difficulties of these calculations.

We were unable to find a stable noncollinear magnetic arrangement of the icosahedron.

3. Spin−Orbit Effects in the Dimer. After including spin−orbit contributions, the total energy becomes a function of the relative orientation between the molecular geometry and spins. Using the relaxed AFM and FM bond lengths for Fe_2 (Table 3), with an *x*-aligned molecule, gives anisotropies in the energy of the order of 14 and 5 meV per atom, respectively (Figure 6a,b). The relative energy between the FM and AFM

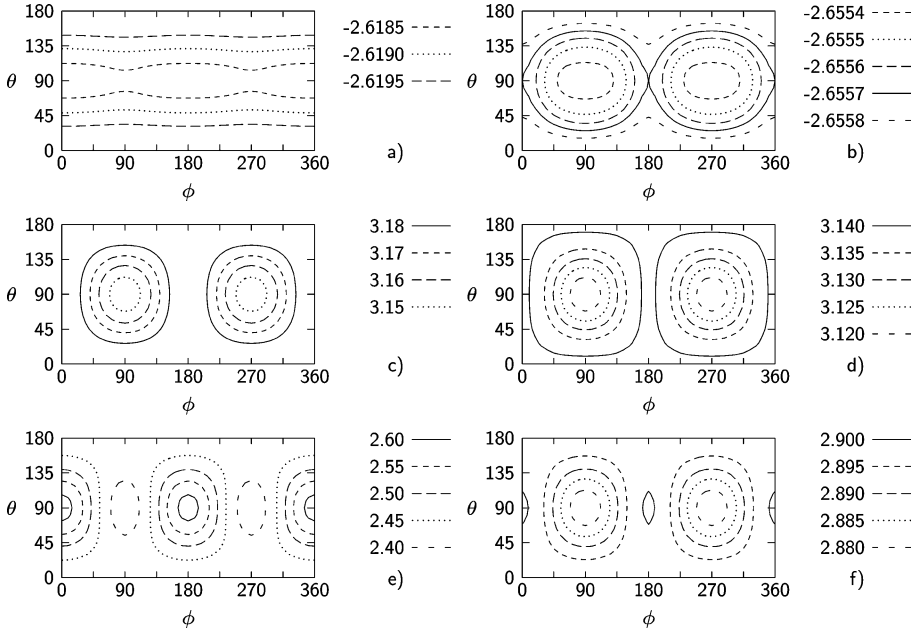

Figure 6. Total energy (Hartree) of *x*-axis aligned Fe_2 including spin−orbit as a function of the orientation of its magnetic moment (angles in degrees with $\theta = 0$ lying along $+z$, and $\theta = \pi/2$, $\phi = 0$ along $+x$) is shown for the (a) AFM and (b) FM states. The per-atom magnitudes of the corresponding spin-only magnetic moments (μ_B) are shown in (c) and (d), respectively. The total magnetic moment per atom (μ_B) including orbital moment is shown in (e) and (f).

structures is unchanged compared with the noncollinear results (0.49 eV per atom in favor of FM). In both cases, the magnetic easy axis is along *z*, and for the FM state, the hard axis is clearly along *y*, while the AFM forms an "easy ridge'' in the *xy* plane. The magnitude of the electron contribution to the spin varies by $\sim 0.02\ \mu_B$ between the hard and easy directions in both cases (Figure 6c,d). In the FM case, the spin moment is larger along the hard axis, while the AFM moment largest along $\pm y$. These moments are then of similar magnitude to the results without spin−orbit coupling (Table 3).

With the inclusion of spin−orbit, orbital momentum is no longer quenched, and this modifies the magnitude of the total magnetic moment. In the FM case, this reduces the total moment by $0.24\ \mu_B$ but does not change the pattern of magnetization with orientation. For the AFM state, however, in addition to a larger reduction of moment per atom of $0.58\ \mu_B$ for the easy axis, the maximum in the magnetization shifts to lie along $\pm x$ with a change of $0.78\ \mu_B$ in the magnitude along that direction compared to the pure spin contribution.

As discussed above for the atom (section 3D), the contribution from the orbital moment is probably underestimated.

4. Summary

We have performed approximate density functional based SDFTB calculations on small iron clusters using a collinear as well as noncollinear description. Generally, we find a good agreement between the SDFTB results and DFT reference results. In agreement with DFT/PAW results, we find a noncollinear ground state for the symmetric Fe_5 cluster, which becomes a ferromagnetic state if the geometrical symmetry is broken. For the Fe_{13} icosahedron, we find in agreement with DFT calculations a ferromagnetic state for large volumes, an antiferromagnetic state for small volumes, and an additional antiferromagnetic state for large cluster volumes depending on the initialization. No noncollinear spin arrangement could be found for this cluster.

The results of the inclusion of spin−orbit coupling for the Fe_2 molecules within the noncollinear SDFTB approach were reported. These demonstrate that it is indeed possible to discern hard and soft magnetic directions although the energy differences are small.

These encouraging results open the possibility to conduct studies on much larger systems than possible with fully self-consistent DFT approaches, especially including noncollinear spin configurations and spin−orbit coupling effects for systems where these become important, i.e., in heavy 4*f* elements.

Acknowledgment. We thank Dr. John McKelvey for his contribution in organizing the DFTB Session at the Fall Meeting 2006 of the American Chemical Society. B.H. acknowledges the Royal Society of Edinburgh BP Research Fellowship for funding.

References and Notes

(1) Porezag, D.; Frauenheim, Th.; Köhler, T.; Seifert, G.; Kaschner, R. *Phys. Rev. B* **1995**, *51*, 12947.

(2) Elstner, M.; Porezag, D.; Jungnickel, G.; Elsner, J.; Haugk, M.; Frauenheim, Th.; Suhai, S.; Seifert, G. *Phys. Rev. B* **1998**, *58*, 7260.

(3) Frauenheim, Th.; Seifert, G.; Elstner, M.; Niehaus, T. A.; Köhler, C.; Amkreutz, M.; Sternberg, M. *J. Phys.: Condens. Matter* **2002**, *14*, 3015.

(4) Frauenheim, Th.; Seifert, G.; Elstner, M.; Hajnal, Z.; Jungnickel, G.; Porezag, D.; Suhai, S.; Scholz, R. *Phys. Status Solidi B* **2001**, *217*, 41.

(5) Köhler, C.; Seifert, G.; Frauenheim, Th. *Chem. Phys.* **2005**, *309*, 23.

(6) Köhler, C.; Seifert, G.; Gerstmann, U.; Elstner, M.; Overhof, H.; Frauenheim, Th. *Phys. Chem. Chem. Phys.* **2001**, *3*, 5109.

(7) Köhler, C.; Seifert, G.; Frauenheim, Th. *Comput. Mater. Sci.* **2006**, *35*, 297.

(8) Köhler, C.; Frauenheim, Th. *J. Comput. Theor. Nanosci.* **2007**, *4*, 1.

(9) Bobadova-Parvanova, P.; Jackson, K. A.; Srinivas, S.; Horoi, M. *Phys. Rev. B* **2003**, *67*, 061202.

(10) Hobbs, D.; Kresse, G.; Hafner, J. *Phys. Rev. B* **2000**, *62*, 11556.

(11) Rollmann, G.; Entel, P.; Sahoo, S. *Comput. Mater. Sci.* **2006**, *35*, 275.

(12) Oda, T.; Pasquarello, A.; Car, R. *Phys. Rev. Lett.* **1998**, *80*, 3622.

(13) Postnikov, A. V.; Entel, P.; Soler, J. M. *Eur. Phys. J. D* **2003**, *25*, 261.

(14) Bobadova-Parvanova, P.; Jackson, K. A.; Srinivas, S.; Horoi, M. *Phys. Rev. B* **2002**, *66*, 195402.

(15) Hobbs, D.; Hafner, J. *J. Phys.: Condens. Matter* **2000**, *12*, 7025.

(16) Knöpfle, K.; Sandratskii, L. M.; Kübler, J. *Phys. Rev. B* **2000**, *62*, 5564.
(17) Sjöstedt, E.; Nordström, L. *Phys. Rev. B* **2002**, *66*, 014447.
(18) Kohn, W.; Hohenberg, P. *Phys. Rev. B* **1964**, *136*, 864.
(19) Kohn, W.; Sham, L. P. *Phys. Rev. A* **1965**, *140*, 1133.
(20) von Barth, U.; Hedin, L. *J. Phys. C* **1972**, *5*, 1629.
(21) Foulkes, W.; Haydock, R. *Phys. Rev. B* **1989**, *39*, 12520.
(22) For the unoccupied 3d shell of Si and S, one actually computes a negative Hubbard *U*.
(23) Nordström, L.; Singh, D. J. *Phys. Rev. Lett.* **1996**, *76*, 4420.
(24) Sticht, J.; Höck, K.-H.; Kübler, J. *J. Phys.: Condens. Matter* **1989**, *1*, 8155.
(25) Pickett, W. *J. Kor. Phys. Soc.* **1996**, *29*, S70.
(26) Hourahine, B.; Köhler, C.; Aradi, B.; Sanna, S.; Frauenheim, T. *J. Phys. Chem. A* **2007**, submitted for publication.
(27) Újfalussy, B.; Wang, X.-D. Nicholson, D.; Stocks, G.; Wang, Y.; Gyorffy, B. *J. Appl. Phys.* **1999**, *85*, 4824.
(28) Wu, Q.; Voorhis, T. *Phys. Rev. A* **2005**, *72*, 024502.
(29) Podolskiy, A. V.; Vogl, P. *Phys. Rev. B* **2004**, *69*, 233101.
(30) Chadi, D. *Phys. Rev. B* **1977**, *16*, 790.
(31) Pastor, G. M.; Dorantes-Dávila, J.; Pick, S.; Dreyssé, H. *Phys. Rev. Lett.* **1995**, *75*, 326.
(32) Rodriguez, C.; Ganduglia-Pirovano, M.; Peltzery Blancá, E.; Petersen, M.; Novák, P. *Phys. Rev. B* **2001**, *63*, 184413.
(33) Nicolas, G.; Dorantes-Dávila, J.; Pastor, G. M. *Phys. Rev. B* **2006**, *74*, 014415.
(34) Cardona, M.; Shaklee, K.; Pollak, F. *Phys. Rev.* **1967**, *154*, 696.
(35) Diéguez, O.; Alemany, M. M. G.; Rey, C.; Ordejón, P.; Gallego, L. J. *Phys. Rev. B* **2001**, *63*, 205407.
(36) Press, M.; Liu, F.; Khanna, S.; Jena, P. *Phys. Rev. B* **1989**, *40*, 399.
(37) Recalculating the magnetic moments with matrix elements obtained from an atomic $3d^6 4s^2$ reference calculation and fixed geometry gives exactly the same results up to Fe_{11} if the different Hubbard *U*'s are taken into account.